CORRECTION POSTED 10 NOVEMBER 2023

SCIENCE ADVANCES | RESEARCH ARTICLE

VIROLOGY

# Human cytomegalovirus UL36 inhibits IRF3-dependent immune signaling to counterbalance its immunoenhancement as apoptotic inhibitor

**Yujie Ren[1,2], An Wang[1,2], Bowen Zhang[1,2], Wenting Ji[1,3], Xiao-Xu Zhu[1,2], Jing Lou[1], Muhan Huang[1], Yang Qiu[1,2], Xi Zhou[1,2,3]***



**Apoptotic inhibition and immune evasion have particular importance to efficient viral infection, while a dilemma often faced by viruses is that inhibiting apoptosis can up-regulate antiviral immune signaling. Herein, we uncovered that in addition to inhibiting caspase-8/extrinsic apoptosis, human cytomegalovirus (HCMV)–encoded UL36 suppresses interferon regulatory factor 3 (IRF3)–dependent immune signaling by directly targeting IRF3 to abrogate IRF3 interaction with stimulator of interferon genes or TANK-binding kinase 1 and inhibit IRF3 phosphorylation/activation. Although UL36-mediated caspase-8/extrinsic apoptosis inhibition enhances immune signaling, the immunosuppressing activity of UL36 counterbalances this immunoenhancing "side effect" undesirable for virus. Furthermore, we used mutational analyses to show that only the wild-type, but not the UL36 mutant losing either inhibitory activity, is sufficient to support effective HCMV replication in cells, showing the functional importance of the dual inhibition by UL36 for the HCMV life cycle. Together, our findings demonstrate a sophisticated mechanism by which HCMV tightly controls innate immune signaling and extrinsic apoptosis for efficient infection.**

## INTRODUCTION

Human cytomegalovirus (HCMV) is an important human pathogen that belongs to the subfamily Betaherpesvirinae in the family Herpesviridae. The large proportion of the global population, with an occurrence of 60 to 100% depending on different socioeconomic and geographical factors, has been infected by this virus (*1*, *2*). HCMV infection is well known for its latency that can persist lifelong after the primary infection. Despite being usually asymptomatic in adults, reactivation from latency can be achieved in certain immunocompromised circumstances, including acquired immunodeficiency syndrome and organ or stem cell transplantations, which can result in significant morbidity or mortality in these people (*2*–*4*). Besides, congenital infections by HCMV are common causes for fetal or neonatal malformations, as approximately 0.5% of total pregnancies in the world are affected by this herpesvirus (*5*). Furthermore, HCMV infection has been associated with some autoimmune diseases and degenerative disorders, probably due to chronic inflammatory response caused by this virus (*6*).

Latency and reactivation of HCMV infection have been believed as an ongoing event, which is sophisticatedly controlled by host antiviral defense mechanisms such as innate immune signaling and apoptosis (*4*, *7*–*9*). The cyclic GMP (guanosine monophosphate)–AMP (adenosine monophosphate) synthase (cGAS) recognizes viral double-stranded DNAs and produce cyclic GMP-AMP, which activates stimulator of interferon genes (STING; also known as MITA/ERIS/MPYS) (*10*–*13*). STING then undergoes homodimerization and binds TANK-binding kinase 1 (TBK1) to phosphorylate and activate interferon regulatory factor 3 (IRF3), leading to the induction of type I interferons (IFN-I) (*14*–*16*). The IFN-I system plays a central role in HCMV-induced host antiviral immune response, while HCMV has been found to use several viral proteins, including UL31, UL42, UL44, UL82, UL83, and UL94, as immune antagonists to inhibit IFN-I signaling pathway (*17*–*24*).

In addition to innate immune signaling, apoptosis is well recognized as an efficient host antiviral defense mechanism, particularly in the early stage of viral infection, by removing infected cells (*25*–*27*). Apoptosis relies on a set of caspases and can be activated via either intrinsic or extrinsic pathway (*28*–*30*). The intrinsic apoptotic pathway is triggered by mitochondrial outer membrane permeabilization, which is caused by some cellular stresses, followed by the release of cytochrome *c* from mitochondria into cytosol, resulting in apoptosome formation, caspase-9 activation, and the subsequent activation of effector caspases-3 and -7 (*31*). The extrinsic apoptotic pathway relies on external induction that activates death receptors, resulting in the activation of initiator caspases-8 and -10 (*32*).

Both intrinsic and extrinsic apoptotic pathways can be induced by viral infection (*26*, *32*). As a slow-replicating virus, HCMV needs the survival of infected cells to establish infection, latency, and reactivation, making inhibition of apoptosis particularly important for this virus (*33*, *34*). It has been reported that HCMV encodes UL37 exon 1 protein (UL37x1) to inhibit intrinsic apoptosis by binding to pro-apoptotic Bax to prevent mitochondrial cytochrome *c* release into cytosols (*35*, *36*). On the other hand, HCMV-encoded UL36, probably better known for its other name, the viral inhibitor of caspase-8 activation (vICA), has been found to inhibit extrinsic apoptosis by directly binding to pro–caspase-8, thereby inhibiting its cleavage into active caspase-8 (*36*, *37*). HCMV encodes UL37x1 and UL36 to function as the respective countermeasures to both intrinsic and extrinsic apoptosis.

It has been previously reported that caspase-8 can inhibit IRF3 activation by cleaving receptor-interacting serine/threonine-protein

[1]State Key Laboratory of Virology, Wuhan Institute of Virology, Chinese Academy of Sciences, Wuhan 430071, China. [2]University of Chinese Academy of Sciences, Beijing 100049, China. [3]School of Life Sciences, Division of Life Sciences and Medicine, University of Science and Technology of China, Hefei, China.
*Corresponding author. Email: zhouxi@wh.iov.cn

kinase 1 (RIP1), which is a signaling enhancer of IRF3 phosphorylation (*38*). Therefore, it is rational to speculate that the expression of HCMV UL36 can enhance the activation of IRF3 by inhibiting caspase-8, resulting in up-regulation of IRF3-dependent immune signaling. However, here, when UL36 was knocked down or overexpressed in HCMV-infected cells, we failed to observe any alteration of phosphorylation of IRF3 or transcription of the immune genes downstream of IRF3. These interesting findings led to the hypothesis that UL36 probably has some immunosuppressive activity. We then uncovered that HCMV UL36 can directly bind to IRF3 to inhibit its interaction with TBK1 and STING, thereby leading to the suppression of IRF3 activation and IRF3-dependent immune signaling, which counterbalances its enhancing effect on IRF3 activation as a caspase-8 inhibitor. Moreover, the dual inhibition of UL36 on both extrinsic apoptosis and IRF3-dependent immune signaling is pivotal for efficient HCMV replication in infected cells.

## RESULTS

### UL36 inhibits HCMV-induced IRF3 activation and downstream immune signaling

HCMV UL36 has been previously reported as an inhibitor of caspase-8 (*37*). Given that caspase-8 can inhibit IRF3 activation by cleaving RIP1, a signaling enhancer of IRF3 phosphorylation (*38*), we speculate that the loss of UL36 expression should reduce the activation of IRF3, resulting in the down-regulation of IRF3-dependent immune signaling during HCMV infection. To this end, we examined the transcription of a series of downstream immune genes, including *IFNB1*, *ISG15*, and *RANTES*, in HCMV-infected human foreskin fibroblasts (HFFs), the permissive cell line for herpesvirus infection, in the presence or absence of UL36-specific siRNAs (fig. S1, A to C). Unexpectedly, compared with control siRNA, the knockdown of HCMV-expressed UL36 failed to reduce the transcription of the immune genes downstream of IRF3 (Fig. 1A).

A rational explanation of such a discrepancy between the speculation and observation is that UL36 may have some immunosuppressive activity, which results in a mutual offset with its potential immunoenhancing effect as a caspase-8/extrinsic apoptosis inhibitor. To test this possibility, z-VAD-FMK, a pan-caspase inhibitor, was used to block apoptosis caused by HCMV infection (fig. S1D and Fig. 1B). In the presence of apoptotic inhibition, knockdown of UL36 effectively enhanced the transcriptional induction of IRF3-dependent immune genes (Fig. 1A) as well as the phosphorylation/activation of IRF3, but not the phosphorylation/activation of TBK1 (Fig. 1C), in HCMV-infected HFFs.

Moreover, we overexpressed UL36 via a lentiviral expression system in HCMV-infected HFFs in the presence or absence of z-VAD-FMK. Our data showed that only under the condition of apoptosis blockade did the overexpression of UL36 dramatically reduce the IRF3 downstream immune signaling (Fig. 1, D and F) as well as the phosphorylation/activation of IRF3, but not TBK1 (Fig. 1, E and G), in HCMV-infected cells.

Together, these results show that when apoptosis is blocked, UL36 inhibited HCMV-induced IRF3 activation and downstream signaling in infected cells, and such an inhibition did not happen at the level of TBK1.

### UL36 interacts with IRF3 to inhibit IRF3-dependent innate immune signaling

To examine whether HCMV UL36 can inhibit DNA-triggered innate immune signaling in the absence of apoptotic inhibition, we assessed the promoter activity of IFN-β, interferon stimulated response element (ISRE), and nuclear factor κB (NF-κB), and the transcription of *IFNB1*, *ISG15*, *RANTES*, *IFNA*, *IL6*, and *TNFA*, in HFFs ectopically expressing cGAS and STING together with UL36. Of note, the transfection of cGAS-STING or DNA ligands did not induce apoptosis (fig. S2). The data showed that the ectopic expression of UL36 inhibited the cGAS-STING-triggered activation of IFN-β, ISRE, and NF-κB promoters as well as the immune gene transcriptions dose-dependently in HFFs (Fig. 2, A and B). In addition, UL36 expression inhibited the transcription of *IFNB1*, *ISG15*, and *RANTES* induced by the transfection of various DNA ligands in cultured HFFs (Fig. 2C). Besides, we further examined the phosphorylation/activation of TBK1 and IRF3 in HFFs treated with these DNA ligands in the presence or absence of UL36 expression. As shown in Fig. 2D, UL36 expression inhibited the DNA-triggered phosphorylation/activation of IRF3 but not TBK1. Thus, our data show that UL36 can inhibit DNA-triggered innate immune signaling in cultured cells.

We then aimed to find out how UL36 inhibits DNA-triggered immune signaling. UL36 efficiently inhibited the activation of ISRE promoter as well as the transcriptional induction of *IFNB1*, *ISG15*, and *RANTES* triggered by the overexpression of cGAS-STING, TBK1, or IRF3, but not IRF3-5D (a constitutively active form of IRF3) (Fig. 3A and fig. S3). Together with our previous observations (Figs. 1, C and G, and 2D), UL36 inhibits the DNA-triggered immune signaling at the level of IRF3.

We then examined whether UL36 interacts with any protein in the immune signaling pathway. Our results showed that UL36 was coimmunoprecipitated with IRF3, but not cGAS, STING, or TBK1 (Fig. 3B). The UL36-IRF3 interaction was further validated via endogenous coimmunoprecipitation using an anti-UL36 antibody in HCMV-infected HFFs (Fig. 3C). Besides, ectopically expressed UL36 has been found to be subcellularly colocalized with IRF3 in cells (Fig. 3D).

To further study the interaction between IRF3 and UL36, we generated a series of IRF3 truncations. The domain mapping analysis and glutathione S-transferase (GST)–pulldown assay suggested that the 197 to 394 amino acids of IRF3 is responsible for interacting with UL36 (Fig. 3G). Additionally, the presence of UL36 substantially impaired the IRF3-TBK1 or IRF3-STING interaction (Fig. 3, H and I), but not the TBK1-STING interaction (Fig. 3J).

Moreover, we assessed the effect of UL36 on the IRF3-TBK1 or IRF3-STING interaction in HCMV-infected HFFs via endogenous coimmunoprecipitation assay. For this purpose, in HCMV-infected HFFs, we stably expressed UL36 via lentivirus, or knocked down endogenous UL36 by RNAi. Our data showed that the overexpression or knockdown of UL36 resulted in substantial reduction or enhancement of the endogenous interactions of IRF3-TBK1 and IRF3-STING, respectively (Fig. 3, K and L), showing that UL36 did inhibit IRF3 interaction with either TBK1 or STING during HCMV infection.

Together, our findings show that HCMV UL36 targets IRF3 to abrogate IRF3-TBK1 and IRF3-STING interaction, resulting in the inhibition of IRF3 activation and IRF3-dependent immune signaling.

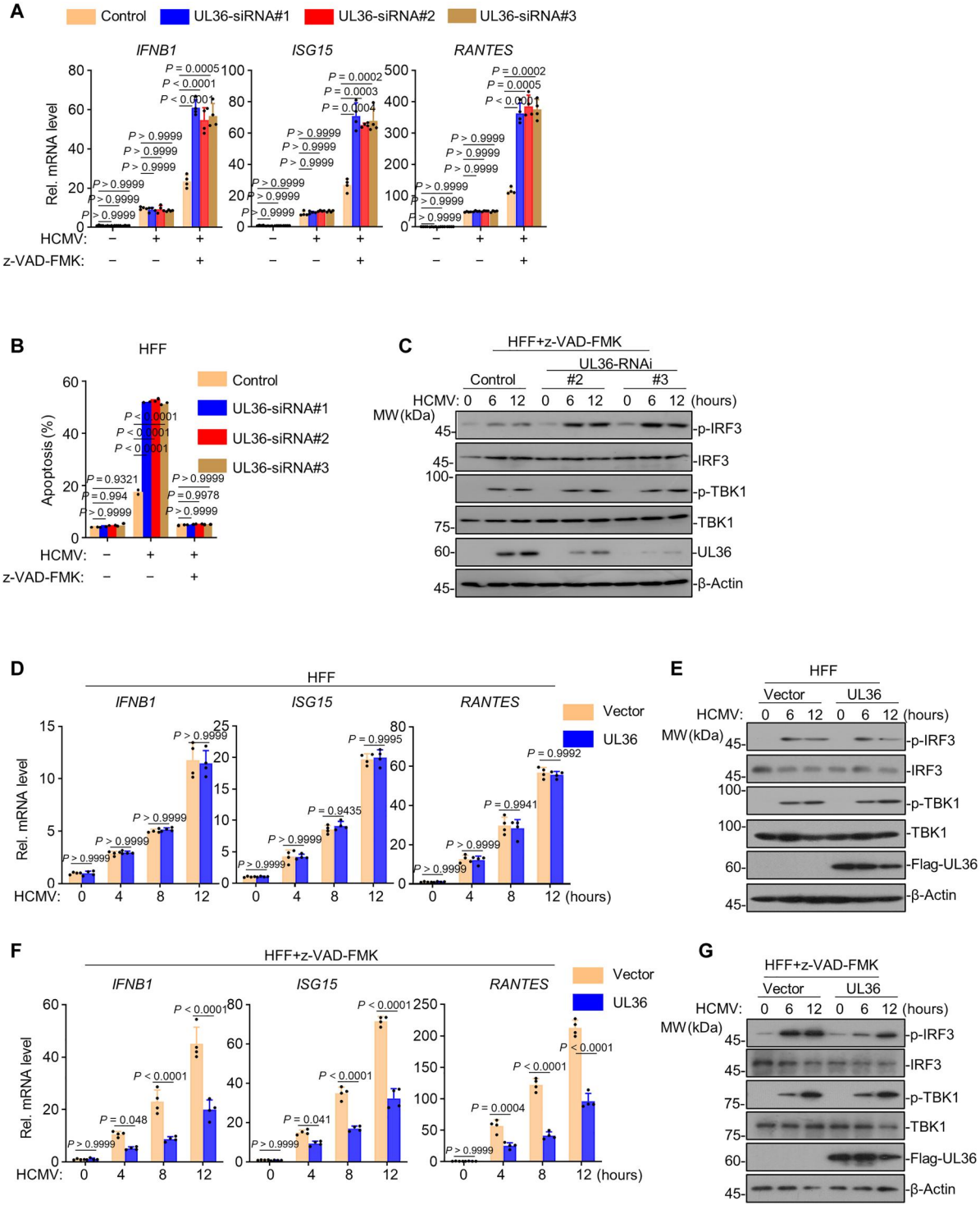


**Fig. 1. UL36 inhibits HCMV-induced IRF3 activation and downstream immune signaling.** (**A** and **B**) HFFs were transfected with siRNAs specifically for UL36 (UL36-siRNA#1, UL36-siRNA#2, or UL36-siRNA#3) or control siRNA (Control) for 24 hours, followed by infection with HCMV (MOI = 1) in the absence or presence of z-VAD-FMK. At 12 hours post-transfection (h.p.t.), qRT-PCR was performed to measure the transcription of indicated antiviral genes (A), cells were collected and stained with annexin V–FITC/PI for flow cytometry analysis, and the percentage of apoptotic cells was measured (B). (**C**) HFFs were transfected and infected as in (A) in the presence of z-VAD-FMK followed by infection with HCMV (MOI = 1). At 12 h.p.i., cell lysates were subject to immunoblots with the indicated antibodies. (**D** to **G**) HFFs stably expressing UL36 or empty vector were infected with HCMV (MOI = 1) in the absence (D and E) or presence (F and G) of z-VAD-FMK. At 0, 4, 8 and 12 h.p.t., qRT-PCR was performed to measure the transcription of indicated antiviral genes (D and F). At 0, 6, and 12 h.p.i., cell lysates were subject to immunoblots with the indicated antibodies (E and G). Immunoblots are representative of three independent experiments. Graphs show mean ± SD ($n$ = 4, biologically independent experiments for A, D, and F or $n$ = 2 for B). Statistical significance was determined by two-way ANOVA in (A), (D), and (F), or one-way ANOVA in (B).

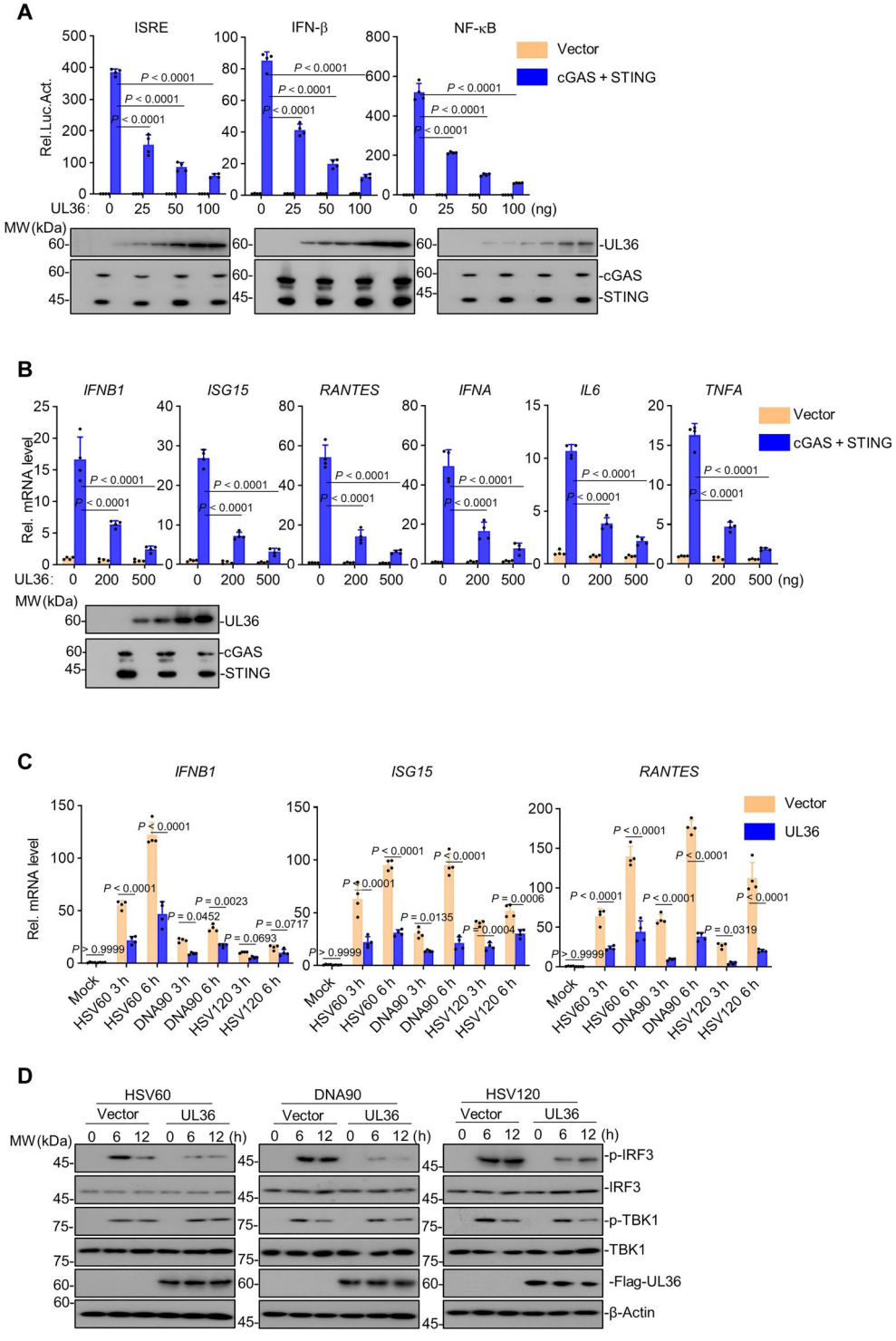


**Fig. 2. UL36 inhibits DNA-triggered IRF3 activation and downstream immune signaling.** (**A**) Top: luciferase reporter assay analyzing IFNβ, ISRE, or NF-κB promoter activity was conducted in HFFs transfected with the plasmids of FLAG-cGAS plus FLAG-STING or an empty vector together with the indicated amounts of FLAG-UL36 expression plasmid for 24 hours. Bottom: blots showing the expression levels of these transfected proteins. (**B**) Top: HFFs were transfected with the plasmids of FLAG-cGAS plus FLAG-STING or an empty vector together with the indicated amounts of FLAG-UL36 expression plasmid for 24 hours, followed by qRT-PCR of the indicated antiviral genes. Bottom: blots showing the expression levels of these transfected proteins. (**C** and **D**) HFFs stably expressing UL36 or empty vector were untreated (mock) or transfected with the indicated DNA ligands (HSV60, DNA90, or HSV120). At 0, 3, and 6 h.p.t., total RNA was extracted and subject to qRT-PCR of indicated antiviral genes (C); at 0, 6, and 12 h.p.t., the cell lysates were prepared and subject to immunoblots with the indicated antibodies. Immunoblots are representative of three independent experiments (D). Graphs show mean ± SD ($n$ = 4 biologically independent experiments). Statistical significance was determined by two-way ANOVA. h, hours.

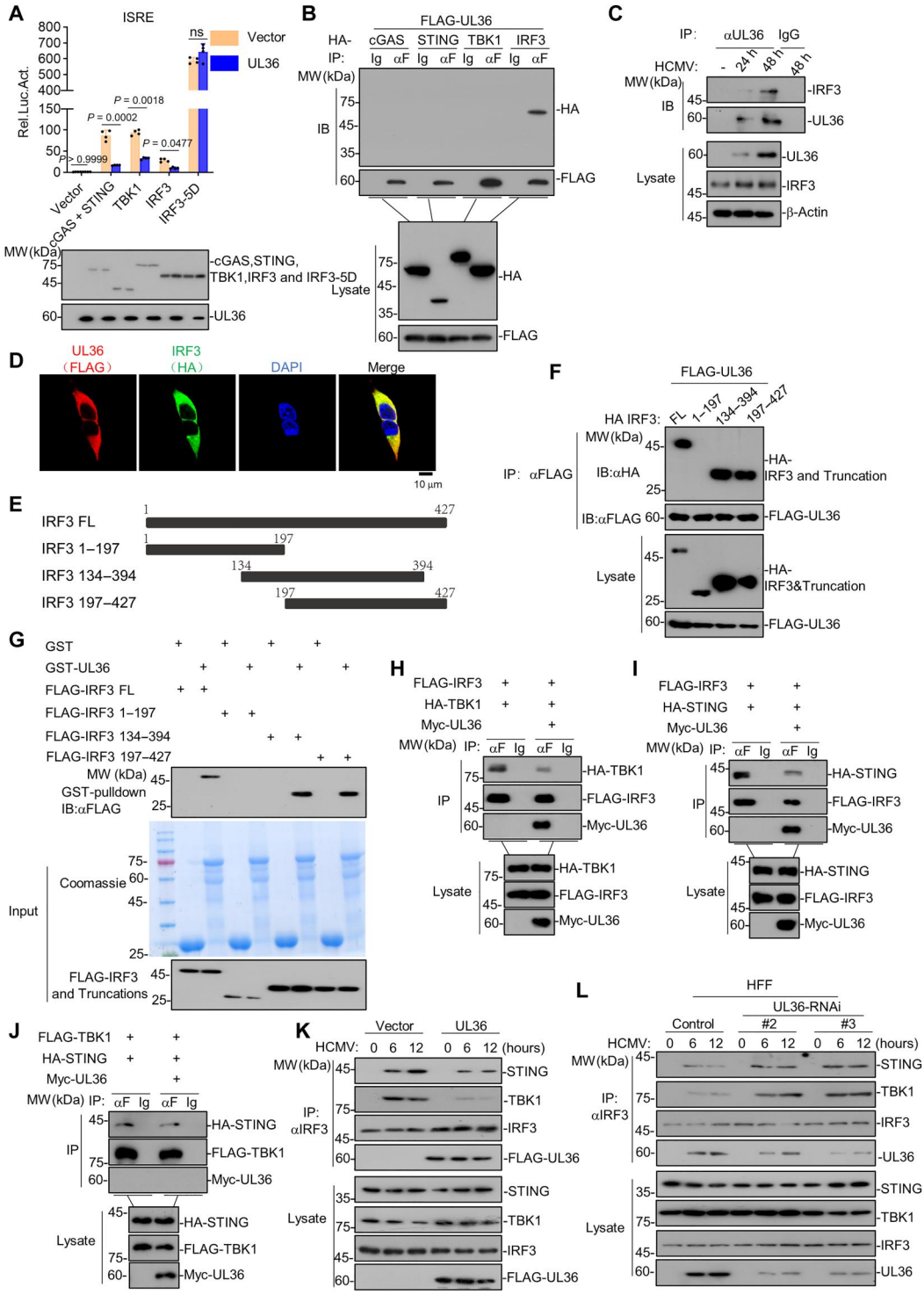


**Fig. 3. UL36 interacts with IRF3 to inhibit IRF3-dependent innate immune signaling.** (**A**) Top: 293T cells were transfected with ISRE reporter and indicated plasmids together with FLAG-UL36 or empty vector for 24 hours before luciferase assay. Bottom: blots showing the expression of indicated proteins. Graph shows mean ± SD ($n$ = 4 biologically independent experiments). Statistical significance was determined by two-way ANOVA. (**B**) 293T cells were transfected with the indicated plasmids together with FLAG-UL36. After 24 hours, cells were subjected to immunoprecipitation (IP) with anti-FLAG antibody or IgG, followed by immunoblots (IB). (**C**) HFFs were infected with HCMV (MOI = 1). At 24 or 48 h.p.i., cells were subject to immunoprecipitation with anti-UL36 antibody or IgG, followed by immunoblots. h, hours. (**D**) 293T cells were transfected with FLAG-UL36 and HA-IRF3. At 24 h.p.t., cells were fixed and stained with anti-FLAG–, anti-HA–, Alexa 488–, and Alexa 594–conjugated IgG antibodies, followed by immunofluorescence. Scale bar, 10 μm. (**E**) The schematic illustration of UL36 truncations. (**F**) 293T cells were transfected with FLAG-UL36 together with HA-IRF3 or indicated truncation. At 24 h.p.t., cell lysates were subject to immunoprecipitation with anti-FLAG antibody, followed by immunoblots. (**G**) Purified GST, GST-UL36, and FLAG-IRF3 or indicated truncation were incubated as indicated. The mixtures were subjected to Coomassie blue staining and immunoblots. The mixtures were subjected to GST pull-down followed by immunoblots. (**H** to **J**) 293T cells were transfected with the indicated plasmids. After 24 hours, cells were subjected to immunoprecipitation with anti-FLAG antibody or IgG, followed by immunoblots. (**K**) HFFs expressing UL36 or empty vector were infected with HCMV (MOI = 1) for 12 hours and then subjected to immunoprecipitation with anti-IRF3 antibody, followed by immunoblots. (**L**) HFFs were transfected with the indicated siRNAs, infected by HCMV (MOI = 1). At 0, 6, and 12 h.p.i., cells were subjected to immunoprecipitation with the anti-IRF3 antibody, followed by immunoblots. Immunoblots are representative of three independent experiments.

### The Ser$^{177}$ of UL36 is required for targeting IRF3

After determining the region of IRF3 responsible for UL36 binding, we aimed to identify the region of UL36 responsible for binding IRF3. Thus, we generated a series of UL36 truncations, and the data showed that $UL36_{FL}$, $UL36_{1–297}$, $UL36_{136–297}$, $UL36_{136–315}$, or $UL36_{136–476}$ but not $UL36_{297–476}$ or $UL36_{316–476}$ interacted with IRF3 (fig. S4, A and B), and only $UL36_{297–476}$ or $UL36_{316–476}$ failed to inhibit the cGAS-STING triggered *IFNB1*, *ISG15*, and *RANTES* transcription (fig. S4C), indicating that the amino acid 136 to 297 region of UL36 is important for IRF3-UL36 interaction. To further identify the key amino acid(s) within UL36 responsible for its immunosuppressing activity, we constructed a set of UL36 deletion mutants within the amino acid 136 to 297 region. Our data showed that $UL36_{\Delta177–189}$ (deleting amino acids 177 to 189 of UL36) completely lost its capability to interact with IRF3 and inhibit the cGAS-STING-triggered *IFNB1* transcription (fig. S4, D and E), showing that the amino acid 177 to 189 region is required for UL36 to interact with IRF3 and antagonize IRF3-dependent immune signaling.

Next, we introduced a series of single-point mutations into the amino acid 177 to 189 region by replacing the serine residue at 177 with threonine (S177T); the isoleucine residue at 178 with alanine (I178A); the aspartic residue at 179, 180, 183, or 187 with alanine (D179A, D180A, D183A, or D187A); the proline residue at 181 or 186 with threonine (P181T or P186T); the phenylalanine residue at 182 with threonine (F182T); the glutamic residue at 184 with alanine (E184A); the cysteine residue at 185 with alanine (C185A); the threonine residue at 188 with alanine (T188A); or the histidine residue at 188 with alanine (H189A). We found that the S177T mutation abolished the capability of UL36 to interact with IRF3 and inhibit the cGAS-STING triggered immune gene transcriptions (Fig. 4, A to C). To provide further mechanistic insight, we then assessed whether the S177T mutation would abolish the inhibitory effects of the IRF3-STING and IRF3-TBK1 interactions. As expected, overexpressing $UL36_{S177T}$ did not inhibit the IRF3-TBK1 or IRF3-STING interaction (Fig. 4, D and E). Consistently, $UL36_{S177T}$ also failed to inhibit the endogenous interaction of IRF3 with TBK1 or STING in HCMV-infected HFFs (Fig. 4F).

Together, these findings demonstrate that the residue S177 of UL36 is essentially required for UL36 to directly target IRF3, abrogate the IRF3-TBK1 and IRF3-STING interactions during HCMV infection, and subsequently inhibit IRF3-dependent immune signaling.

### The immunosuppression by UL36 counterbalances the immunoenhancing effect of its anti-apoptotic activity

Previous studies reported that apoptotic inhibition by UL36 requires the Cys$^{131}$ (C131) residue of UL36 (*37*). To assess the contributions of the S177 and C131 residues on the functions of this viral protein, we first constructed UL36-deficient HCMV ($HCMV_{\Delta UL36}$) via CRISPR-Cas9 based on the $HCMV_{Towne}$ strain Towne. $HCMV_{\Delta UL36}$ was successfully recovered and used to infect HFFs at a multiplicity of infection (MOI) of 1 (fig. S5A). We then stably expressed the wild-type UL36 or its mutants, $UL36_{S177T}$, $UL36_{C131R}$, and $UL36_{C131R\&S177T}$, in HFFs, followed by infection with $HCMV_{\Delta UL36}$. After that, we examined the effect of wild-type or different UL36 mutants on apoptosis. As expected, $UL36_{WT}$ or immunosuppression-deficient $UL36_{S177T}$, but not $UL36_{C131R}$ or $UL36_{C131R\&S177T}$, retained the ability to inhibit $HCMV_{\Delta UL36}$-induced apoptosis in HFFs (Fig. 5A). In addition, similar to that of wild-type UL36, ectopic expression of the anti-apoptosis–deficient mutant $UL36_{C131R}$ effectively inhibited the cGAS-STING-triggered activation of IFN-β, ISRE, and NF-κB promoters as well as immune gene induction (Fig. 5, B and C). Thus, the immunosuppressing and anti-apoptotic activities of UL36 are functionally independent from each other.

Compared with empty vector, anti-apoptosis–deficient $UL36_{C131R}$ but not wild-type UL36 effectively inhibited immune gene induction, cytokine secretion, or IRF3 phosphorylation in $HCMV_{\Delta UL36}$-infected HFFs (Fig. 5, D and F, and fig. S5C). $UL36_{C131R}$ cannot inhibit apoptosis but keeps its immunosuppressing activity (Fig. 5, A to C). Thus, the stronger suppressing activity of $UL36_{C131R}$ than that of wild-type UL36 on $HCMV_{\Delta UL36}$-triggered immune gene induction, cytokine secretion, or IRF3 activation should be attributed to apoptosis-mediated immunosuppressing effect, as the UL36-mediated apoptotic inhibition was lifted. Consistently, when apoptosis is blocked by pan-caspase inhibitor z-VAD-FMK, $UL36_{WT}$ and $UL36_{C131R}$ showed similar effect in immunosuppression during viral infection (Fig. 5, E and G, and fig. S5, B and D).

Otherwise, $HCMV_{\Delta UL36}$ infection induced even higher levels of immune gene induction, cytokine secretion, or IRF3 phosphorylation in the presence of $UL36_{S177T}$ when being compared with that of empty vector in HFFs (Fig. 5, D and F, and fig. S5C). $UL36_{S177T}$ loses its immunosuppressing activity but can still inhibit apoptosis (Figs. 4 and 5A). Hence, this result indicates that the immunoenhancing effect of $UL36_{S177T}$ was owing to its anti-apoptotic activity, which was further confirmed by the observation that compared with that of empty vector, $UL36_{S177T}$ showed a similar effect on immune signaling when apoptosis was blocked by z-VAD-FMK (Fig. 5, E and G, and fig. S5, B and D). In addition, compared with that of empty vector, the double-point mutant $UL36_{C131R\&S177T}$, which loses both immunosuppressing and anti-apoptotic activities, showed a similar effect on immune gene induction in either the presence or the absence of z-VAD-FMK (Fig. 5, D and E).

It is noteworthy that the approach of ectopically expressing UL36 in cells before HCMV infection has the potential limitation that the pre-existence of UL36 may affect certain signaling pathway(s) or other earlier viral gene expression in cells. Therefore, we used a Tet-On doxycycline-inducible system to express UL36 or its mutants in HFFs after $HCMV_{\Delta UL36}$ infection (fig. S5E). Our data show that when being expressed either before or after $HCMV_{\Delta UL36}$ infection, UL36 or its distinct mutant had the same effect on IRF3 immune signaling (Fig. 5D and fig. S5F), excluding the possible interference of pre-existing UL36 before HCMV infection.

Moreover, previous studies of HCMV UL36 and its ortholog M36 in murine HCMV had found that these viral proteins had more pronounced effects in macrophages than in fibroblasts (*39*–*43*). Thus, we examined the effects of UL36 or its mutants on immune gene induction in THP1-derived macrophages, and the results are consistent with our previous observations in HFFs (fig. S5, G and H, and Fig. 5, D and E).

To provide some mechanistic insight into how UL36 works, we assessed the effects of different UL36 mutants on the STING-IRF3 or TBK1-IRF3 interaction in the context of $HCMV_{\Delta UL36}$ infection. Our data showed that similar to $UL36_{WT}$, $UL36_{C131R}$ disrupted IRF3

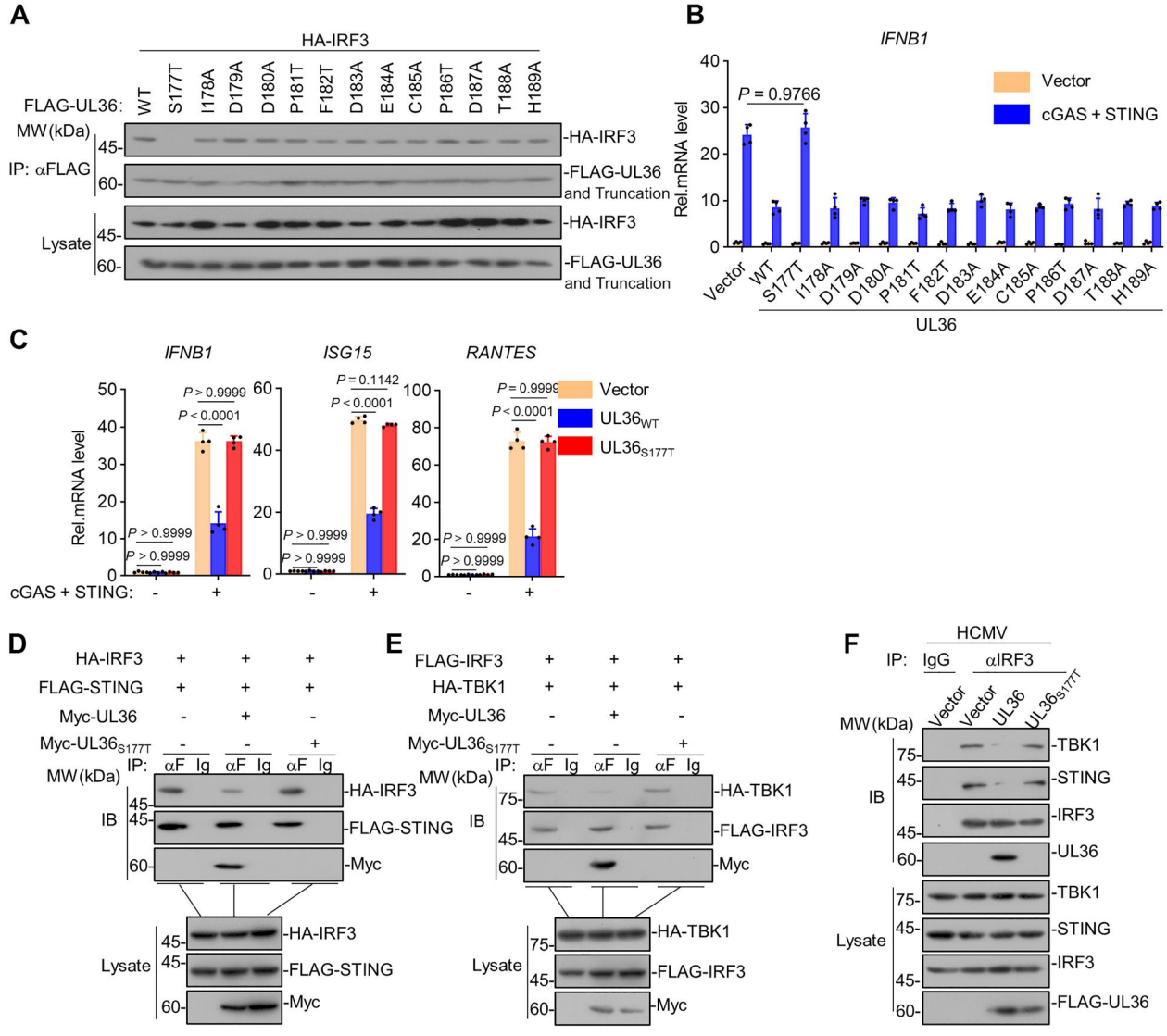


**Fig. 4. The Ser$^{177}$ of UL36 is required for targeting IRF3.** (**A**) 293T cells were transfected with the plasmid of HA-IRF3 together with the plasmid of FLAG-UL36 or the indicated mutant. After 24 hours, cell lysates were subjected to immunoprecipitation with anti-FLAG antibody, followed by immunoblots with anti-FLAG and anti-HA antibodies. (**B**) 293T cells were transfected with the plasmids of FLAG-cGAS plus FLAG-STING together with the plasmids of FLAG-UL36 or the indicated mutant for 24 hours, followed by qRT-PCR of *IFNB1*. The transfection of the empty vector was used as a negative control. (**C**) 293T cells were transfected with or without the plasmids of FLAG-cGAS plus FLAG-STING together with the plasmids of FLAG-UL36 or FLAG-UL36$_{S177T}$ for 24 hours. Total RNAs were extracted and subjected to qRT-PCR of the indicated antiviral genes. (**D** and **E**) 293T cells were transfected with the indicated plasmids. After 24 hours, cells were subjected to immunoprecipitation with anti-FLAG antibody or IgG, followed by immunoblots with anti-FLAG, anti-HA, and anti-Myc antibodies. (**F**) HFFs stably expressing UL36, UL36$_{S177T}$, or empty vector were infected with HCMV (MOI = 1). At 12 h.p.i., cell lysates were subjected to immunoprecipitation with anti-IRF3 antibody or IgG, followed by immunoblots with the indicated antibodies. Immunoblots are representative of three independent experiments. Graph shows mean ± SD ($n$ = 4 biologically independent experiments). Statistical significance was determined by two-way ANOVA.

interaction with STING or TBK1, while the immunosuppression-deficient UL36$_{S177T}$ failed to do so (Fig. 6A).

UL36 is a well-recognized caspase-8 inhibitor, and it has been previously reported that blocking caspase-8 can cause up-regulation of IRF3 phosphorylation, which was confirmed in this study by using the caspase-8-specific inhibitor z-IETD-FMK (Fig. 6, B and C, and fig. S6A). Moreover, in the presence of z-IETD-FMK, UL36$_{WT}$ but not UL36$_{S177T}$ effectively inhibited the up-regulation of IRF3 phosphorylation (Fig. 6, B and C). Furthermore, we examined the effect of UL36 on IRF3 activation in the absence or presence of distinct caspase inhibitor, including pan-caspase inhibitor z-VAD-FMK, caspase-8-specific z-IETD-FMK, or caspase-9–specific z-LEHD-FMK. Of note, UL36 showed further inhibition on apoptosis only in the presence of z-LEHD-FMK but not z-IETD-FMK (fig. S6, A and B), confirming the apoptosis-inhibition specificities of UL36 as well as these caspase inhibitors. Our data showed that the loss of UL36 expression in HCMV-infected cells (i.e., HCMV$_{\Delta UL36}$ infection) resulted in the substantial up-regulation of IRF3 phosphorylation in the presence of either pan-caspase or caspase-8-specific inhibitor, but not the presence of

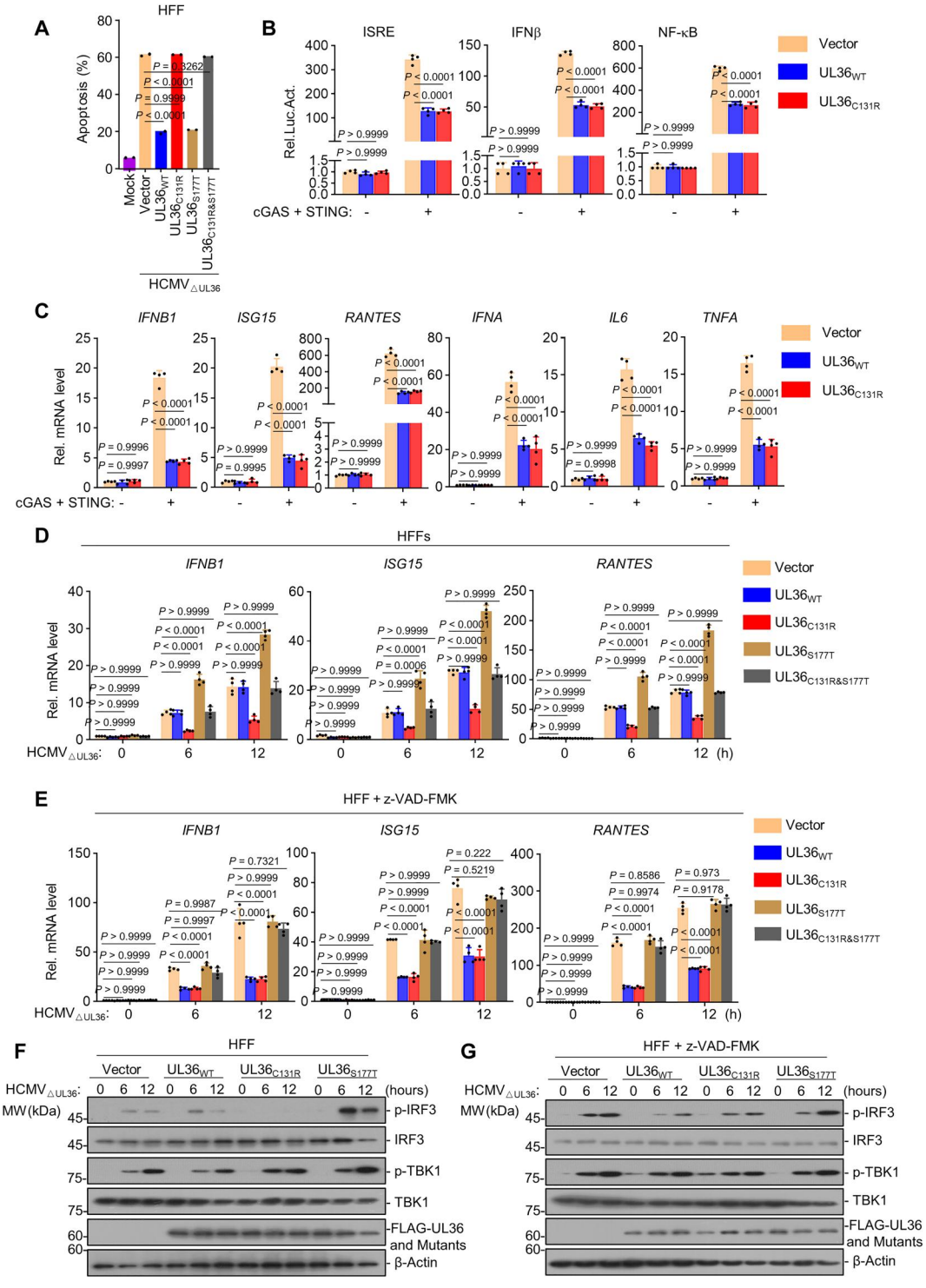


**Fig. 5. The immunosuppression by UL36 counterbalances the immunoenhancing effect of its anti-apoptotic activity.** (**A**) HFFs stably expressing UL36, $UL36_{C131R}$, $UL36_{S177T}$, $UL36_{C131R\&S177T}$, or empty vector were uninfected or infected with $HCMV_{\Delta UL36}$ (MOI = 1). At 12 h.p.i., cells were collected and stained with annexin V–FITC/PI for flow cytometry analysis and the percentage of apoptotic cells was measured. (**B**) Luciferase reporter assay analyzing IFNβ, ISRE, or NF-κB promoter activity was conducted in 293T cells transfected with or without the plasmids of FLAG-cGAS plus FLAG-STING together with the plasmid of FLAG-UL36 or FLAG-$UL36_{C131R}$ for 24 hours. (**C**) 293T cells were transfected with or without the plasmids of FLAG-cGAS plus FLAG-STING together with the plasmid of FLAG-UL36 or FLAG-$UL36_{C131R}$ for 24 hours. Total RNAs were extracted and subject to qRT-PCR of the indicated antiviral genes. (**D** and **E**) HFFs stably expressing UL36, $UL36_{C131R}$, $UL36_{S177T}$, $UL36_{C131R\&S177T}$, or empty vector were uninfected or infected with $HCMV_{\Delta UL36}$ (MOI = 1) in the absence (C) or presence (D) of z-VAD-FMK. At 0, 6, and 12 h.p.i., qRT-PCR was performed to measure the transcription of indicated antiviral genes. (**F** and **G**) HFFs stably expressing UL36, $UL36_{C131R}$, $UL36_{S177T}$, or empty vector were uninfected or infected with $HCMV_{\Delta 36}$ (MOI = 1) in the absence (F) or presence (G) of z-VAD-FMK. At 0, 6, and 12 h.p.i., cell lysates were subjected to immunoblots with the indicated antibodies. Immunoblots are representative of three independent experiments. Graph shows mean ± SD [$n = 4$ biologically independent experiments for (B) to (E) or $n = 2$ for (A)]. Statistical significance was determined by two-way ANOVA in (B) to (E), or one-way ANOVA in (A).

caspase-9–specific inhibitor (Fig. 6, D to G). Therefore, these results indicate that the immunosuppressing activity of UL36 specifically neutralized the immunoenhancing effect caused by caspase-8 inhibition.

Together, our findings show that during HCMV infection, UL36 can simultaneously confer both immunosuppressing and anti-apoptotic functions, which are functionally independent with each other, and the immunosuppression mediated by UL36 counterbalances the immunoenhancing effect of caspase-8 inhibition mediated by the same viral protein.

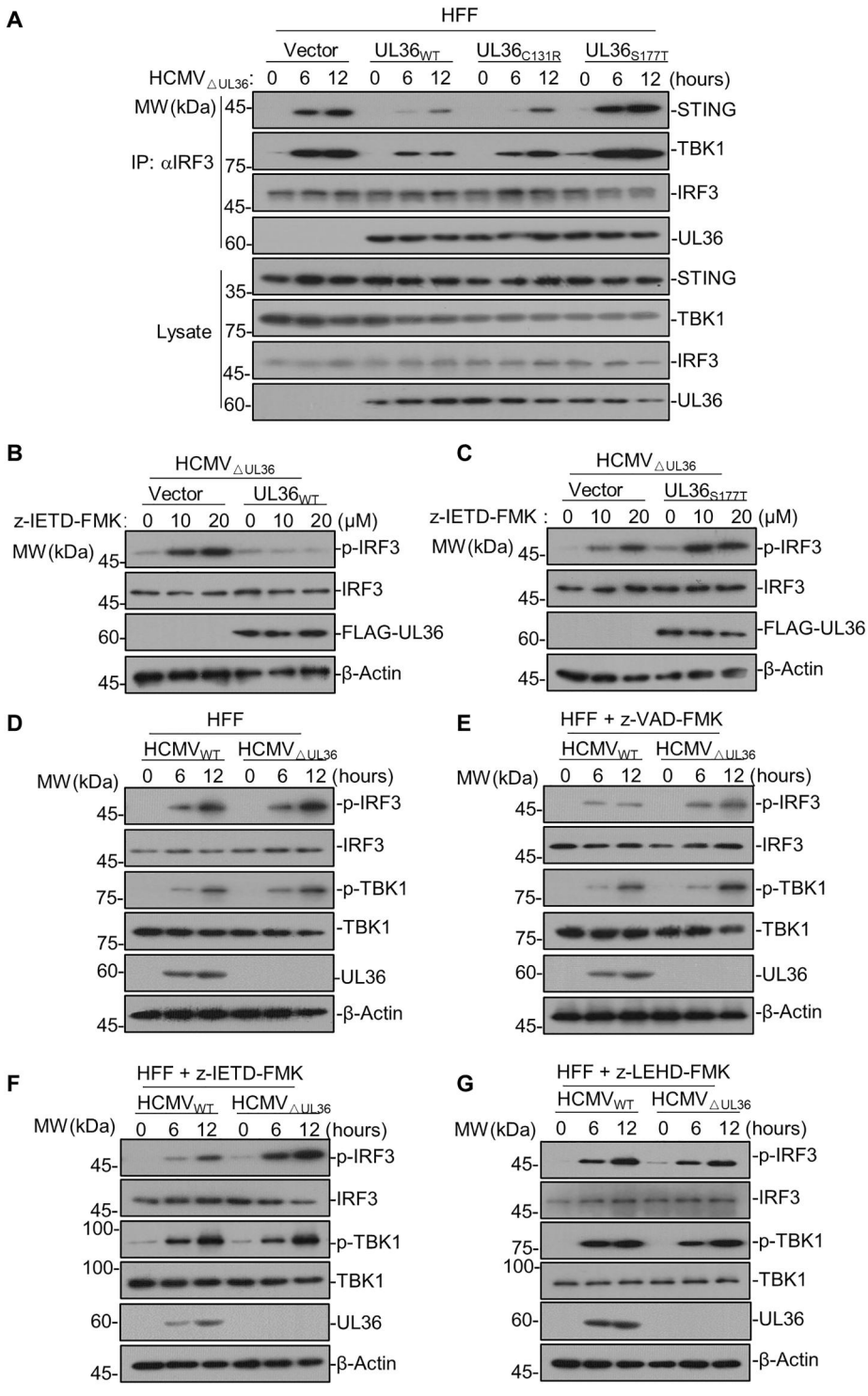


**Fig. 6. UL36 suppresses the immunoenhancing effect caused by its inhibition on caspase-8.** (**A**) HFFs stably expressing UL36, $UL36_{C131R}$, $UL36_{S177T}$, or empty vector were uninfected or infected with $HCMV_{\Delta UL36}$ (MOI = 1). At 0, 6, and 12 h.p.i., cell lysates were subjected to immunoprecipitation with anti-IRF3 antibody, followed by immunoblots with the indicated antibodies. (**B** and **C**) HFFs stably expressing $UL36_{WT}$ (B), $UL36_{S177T}$ (C), or empty vector were infected with $HCMV_{\Delta UL36}$ (MOI = 1) in the absence or presence of z-IETD-FMK (10 μM or 20 μM). At 12 h.p.i., cell lysates were subject to immunoblots with the indicated antibodies. (**D** to **G**) HFFs were infected with HCMV or $HCMV_{\Delta UL36}$ (MOI = 1) in the absence (D) or presence of z-VAD-FMK (E), z-IETD-FMK (F), or z-LEHD-FMK (G). At 0, 6, and 12 h.p.i., cell lysates were subject to immunoblots with the indicated antibodies. Immunoblots are representative of three independent experiments.

### Both the immunosuppressing and anti-apoptotic activities of UL36 are critical for HCMV replication

To further study the functional importance of the dual inhibitory function of HCMV UL36 on both innate immunity and apoptosis, we assessed how losing either immunosuppressing or anti-apoptotic activity, or both, affects the replication of HCMV. For this purpose, $HCMV_{\Delta UL36}$ was used to infect HFFs or THP1-derived macrophages ectopically expressing wild-type or distinct UL36 mutant via the lentiviral or Tet-On doxycycline-inducible system as indicated, followed by assessing viral replication via measuring the expression levels of HCMV genes, including *IE1*, *IE2*, and *pp65*, or the 50% tissue culture infectious dose ($TCID_{50}$), at 96 hours post-infection (h.p.i.) (Fig. 7, A and B, and fig. S7, A to C). Our data show that compared with that of empty vector, restoring $UL36_{WT}$ expression substantially enhanced the viral replication in $HCMV_{\Delta UL36}$-infected cells, while the expression of either $UL36_{C131R}$ or $UL36_{S177T}$ only partially restored viral replication.

Moreover, similar experiments were performed in the presence of distinct caspase inhibitors. In the presence of either pan-caspase inhibitor z-VAD-FMK or caspase-8-specific inhibitor z-IETD-FMK, the expression of anti-apoptosis–deficient $UL36_{C131R}$ showed a similar effect on enhancing the replication of $HCMV_{\Delta UL36}$ compared with that of $UL36_{WT}$, while the immunosuppression-deficient $UL36_{S177T}$ failed to increase viral replication compared with empty vector (Fig. 7, C to F, and fig. S7, D and E). In contrast, the effect of wild-type or distinct UL36 mutant on $HCMV_{\Delta UL36}$ replication showed a similar pattern between that in the presence of caspase-9–specific z-LEHD-FMK or in the absence of any caspase inhibitor (Fig. 7, G and H vs. Fig. 7, A and B), highlighting that the functional importance of UL36 depends on its specific inhibition on caspase-8.

Furthermore, we assessed the effect of wild-type or distinct UL36 mutant on viral replication in the context of abrogating cGAS-STING signaling in HFFs. Our data showed that in cells with the deficiency of either STING or cGAS, the expression of immunosuppression-deficient $UL36_{S177T}$ showed a similar effect on enhancing the replication of $HCMV_{\Delta UL36}$ compared with that of $UL36_{WT}$, while the anti-apoptosis–deficient $UL36_{C131R}$ failed to increase viral replication compared with empty vector (fig. S8).

In conclusion, our findings demonstrate that the inhibitory activities on both IRF3-dependent immune signaling and extrinsic apoptosis/caspase-8 are pivotal for the efficient replication of HCMV.

## DISCUSSION

Viral infections can induce both extrinsic and intrinsic apoptosis, resulting in the removal of infected cells from host organisms (*44*, *45*). As countermeasures, viruses use various strategies, particularly by encoding diverse apoptotic inhibitors, to antagonize both apoptotic pathways (*27*, *46*). For HCMV, the viral protein UL36 has long been found to antagonize extrinsic apoptosis by directly binding pro–caspase-8 to prevent cleavage into active caspase-8, which makes UL36 being named vICA as well (*37*). On the other hand, caspase-8 has been reported to inhibit IRF3 activation by mediating the cleavage of RIP1, while inhibition of caspase-8 can lead to enhanced phosphorylation/activation of IRF3 (*38*). Therefore, a rational speculation is that the inhibition of caspase-8/extrinsic apoptosis should induce IRF3 activation as well as downstream IRF3-dependent immune signaling; such an induction of innate antiviral immunity would inevitably lead to a detrimental intracellular microenvironment for HCMV infection and replication.

However, our initial experiments by either knocking down or overexpressing UL36 in HCMV-infected cells led to an unexpected but very interesting result that neither knockdown nor overexpression of UL36 showed any impact on IRF3 activation or immune signaling. Our further studies revealed that in addition to its anti-apoptotic activity, HCMV UL36 can inhibit IRF3-dependent immune signaling by directly targeting IRF3 to abrogate IRF3 interaction with STING or TBK1 and inhibit IRF3 activation, thereby leading to the suppression of IRF3-dependent immune signaling. Considering that inhibition of caspase-8 by UL36 can lead to IRF3 activation, directly targeting IRF3 itself before its activation and nuclear translocation, rather than some upstream factors, is an ideal way to block the downstream immune signaling (Fig. 8).

We then took advantage of different UL36 mutants that lose either the anti-apoptotic or immunosuppressing activity, or both. We find that the two inhibitory activities of UL36 are mediated by different regions/residues within UL36 and are functionally independent. Besides, the anti-extrinsic apoptosis/caspase-8 activity of UL36 does cause the up-regulation of IRF3 activation and downstream signaling, which can be effectively counterbalanced by the immunosuppressing activity of the same viral protein during HCMV infection. These findings also provide the explanation about why overexpressing or knocking down UL36 was unable to show either immunoenhancing or immunosuppressing effect in HCMV-infected cells, as the effects of these two activities were mutually neutralized. On the other hand, although the mutual neutralization makes the effect of UL36 on immune signaling inevident, only the wild-type, but not UL36 mutant losing either activity, was sufficient to support effective HCMV replication in cells, highlighting the functional importance of the dual inhibition of UL36 on both extrinsic apoptosis and IRF3-dependent immune signaling.

Our previous study has found that the HCMV-encoded UL37x1 protein can simultaneously inhibit both intrinsic apoptosis and innate immunity (*47*). The inhibition of apoptosis is of particular importance for HCMV to establish infection and latency. Therefore, the same virus encodes two distinct viral proteins, UL36 and UL37x1, to respectively inhibit extrinsic and intrinsic apoptotic pathways. UL36 and UL37x1 can confer immunosuppressing activities by directly targeting IRF3 and TBK1, respectively, and these immunosuppression efficiently counterbalance the corresponding immunoenhancing "side effects" caused by their different anti-apoptotic activities, thereby ensuring a balanced, favorable intracellular microenvironment for HCMV life cycle.

HCMV UL36 and its ortholog proteins belong to the US22 family of herpesviral proteins, and $Cys^{131}$ and $Ser^{177}$, the key residues for inhibiting caspase-8 and IRF3 activations, respectively, are conserved within multiple HCMV strains, including the strain Towne used in the current study and other commonly used strains like Merlin (*37*, *41*). On the other hand, a highly passaged, laboratory-adapted HCMV strain AD169 ($HCMV_{AD169}$) bears the C131R mutation within UL36, which makes $HCMV_{AD169}$-UL36 incapable of binding pro–caspase-8 and inhibiting extrinsic apoptosis (*37*); this UL36 protein also contains the S177T mutation, making it defective in binding IRF3 and suppressing IRF3-dependent immune signaling. These findings imply that the anti-apoptotic and immunosuppressing activities of HCMV UL36 are tightly

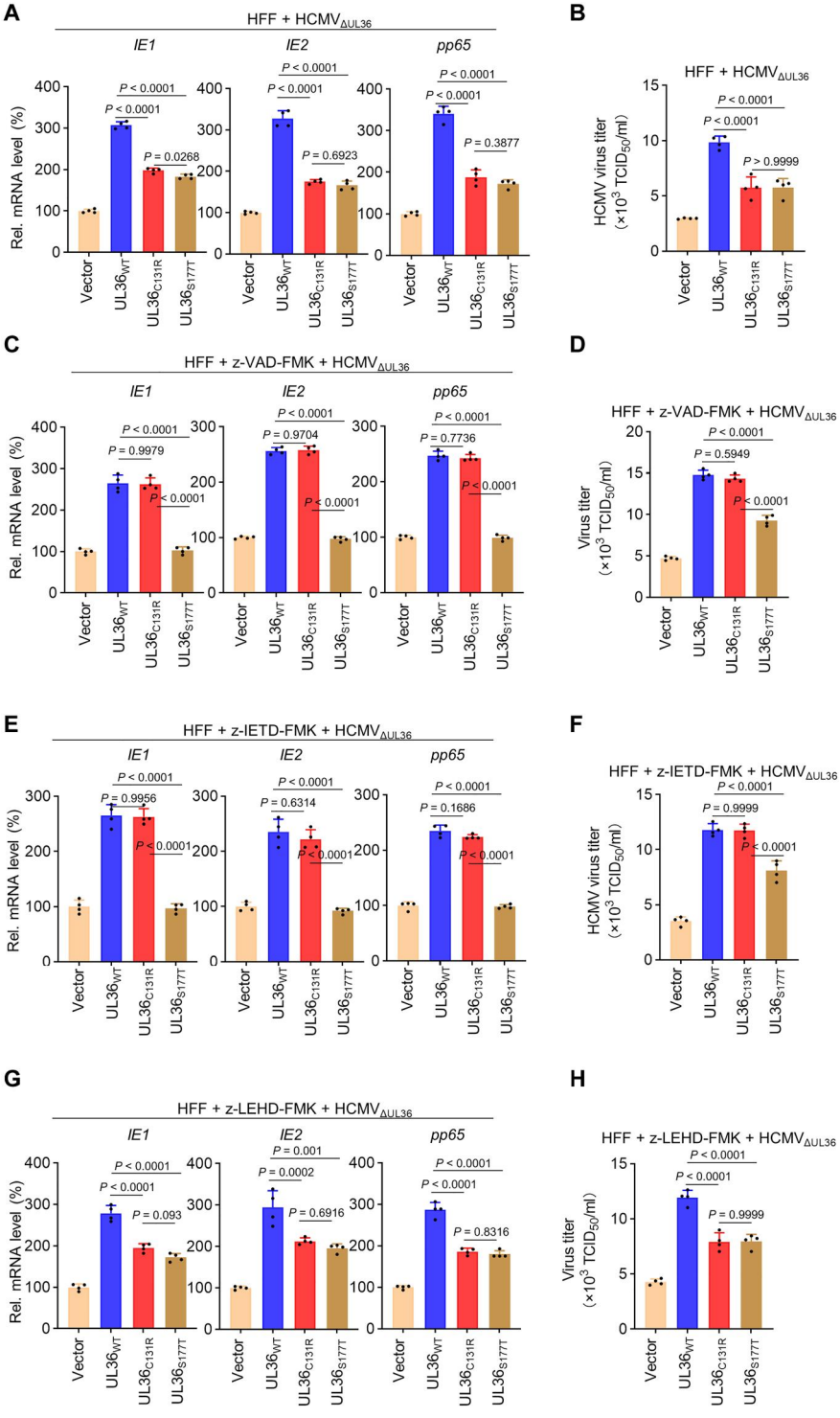


**Fig. 7. Both the immunosuppressing and anti-apoptotic activities of UL36 are critical for HCMV replication.** (**A** to **H**) HFFs stably expressing UL36, UL36$_{C131R}$, UL36$_{S177T}$, or empty vector were infected with HCMV$_{\Delta UL36}$ (MOI = 1) in the absence (A and B) or presence of z-VAD-FMK (C and D), z-LEHD-FMK (E and F), or z-IETD-FMK (G and H). At 96 h.p.i., the mRNA levels of the indicated HCMV genes in HFFs were measured by qRT-PCR (A, C, E, and G), and supernatants were harvested for measurements of the viral titers with standard TCID$_{50}$ assays (B, D, F, and H). Graph shows mean ± SD ($n$ = 4 biologically independent experiments). Statistical significance was determined by one-way ANOVA.

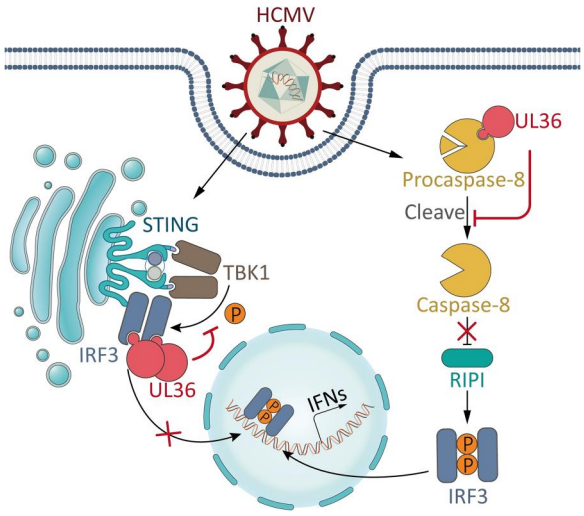


**Fig. 8. Model for the dual inhibition of IRF3-dependent innate immune and caspase-8/extrinsic apoptosis by HCMV UL36.** Caspase-8 can inhibit IRF3 phosphorylation/activation by cleaving RIP1, while HCMV-expressed UL36 directly binds to pro–caspase-8 to prevent its cleavage into active caspase-8, thereby enhancing IRF3 phosphorylation/activation. On the other hand, UL36 can directly target IRF3 to inhibit its interaction with TBK1 or STING, resulting in the suppression of IRF3 activation and downstream immune signaling. This immunosuppressing activity of UL36 counterbalances the immunoenhancing "side effect" of UL36's anti-extrinsic apoptosis/caspase-8 activity.

interlocked in functionalities, suggesting that these two functions face the same set of intracellular pressures (i.e., host antiviral defenses including apoptosis and innate immunity), which further emphasizes the functional importance of this dual inhibitory mechanism. In addition to inhibiting extrinsic apoptosis, UL36 has been reported to inhibit necroptosis by mediating the degradation of mixed lineage kinase domain-like protein (MLKL), a terminal mediator of necroptosis, and this anti-necroptotic activity is mediated by the same residue $Cys^{131}$ responsible for anti-apoptosis (*8*). Hence, UL36 is a multifunctional inhibitor for virus-induced cell death and innate immunity, which is pivotal for HCMV life cycle.

Immune evasion has particular importance for viruses to establish and maintain infection, and multiple HCMV-encoded proteins, including UL31, UL37x1, UL42, UL44, UL82, UL83, and UL94, have been reported to inhibit host innate immunity by targeting different components of immune signaling pathways (*17*–*22*, *47*). In particular, similar to UL36, HCMV UL44 has been shown to interact with and suppress IRF3 (*19*). In the presence of various HCMV proteins with the capability of suppressing immune signaling and even targeting IRF3 itself, it is intriguing to ask for the reason why HCMV uses a single protein, UL36, to confer such a dual suppression. It is probable that HCMV must assure a synchronous counterbalance for the immunoenhancing "side effect" of anti-extrinsic apoptosis/caspase-8, and the integration of the two inhibitory activities in one viral protein provides such an edge for HCMV.

Diverse viruses including herpesviruses, flaviviruses, poxviruses, and enteroviruses have been found to use different strategies to inhibit apoptosis (*48*–*53*). Therefore, how to overcome the inevitable immunoenhancing "side effect" caused by apoptotic inhibition should be serious challenges for most viruses, and it would be intriguing to find out how these viruses reach the balance between anti-apoptosis and immune evasion. In conclusion, this study uncovers that HCMV UL36 directly targets IRF3 to inhibit its activation as well as downstream IRF3-dependent immune signaling. Such an immunosuppression by UL36 counterbalances its immunoenhancing effect as an inhibitor of caspase-8, and the dual inhibition of UL36 on both extrinsic apoptosis and IRF3-dependent immune signaling is pivotal for efficient HCMV replication. These findings demonstrate that HCMV uses a sophisticated strategy to precisely control and balance anti-apoptosis and immune evasion, which extends the knowledge about the immunomodulatory arsenals used by HCMV to establish infections, and sheds light onto developing potential therapies against this notorious virus.

## MATERIALS AND METHODS

### Cell culture

293T cells were commercially obtained from the American Type Culture Collection (ATCC). HFFs were kindly provided by Y.-Y. Wang (Wuhan, Hubei). MRC5 cells were generously provided by the National Virus Resource Center, Wuhan Institute of Virology, Chinese Academy of Sciences (CAS). These cell lines were cultured in Dulbecco's modified Eagle's medium (Gibco, A4192101) containing 10% fetal bovine serum (FBS) (Gibco, 10099141 C) and 1% streptomycin-penicillin (Gibco, 15140122) at 37°C in a $CO_2$ incubator.

THP-1 cells were commercially obtained from the ATCC and cultured in RPMI 1640 (Gibco, 11875119) containing 10% FBS (Gibco, 10099141 C) and 1% streptomycin-penicillin (Gibco, 15140122) at 37°C in a $CO_2$ incubator. To obtain THP-1–derived macrophages, THP-1 cells were treated with phorbol myristate acetate (PMA; Merck, 16561-29-8) at a final concentration of 50 ng/ml.

### Viruses

HCMV (Towne strain) was provided by the National Virus Resource Center, Wuhan Institute of Virology, CAS. HCMV stock was prepared on MRC5 cells, and the virus titer was determined by standard $TCID_{50}$ assays. HCMV (MOI = 2) infected THP-1–derived macrophages in the presence of PMA (50 ng/ml) and 5 mM hydrocortisone (MCE, HY-N0583). Cells were harvested at the indicated h.p.i. for further analysis.

### CRISPR/Cas9-mediated genome editing of HCMV

Potential guide RNAs (gRNAs) targeting UL36 gene were analyzed using the CRISPR Design tool. Double-stranded oligos were cloned into the lentiCRISPRv2 vector and cotransfected with packaging plasmids into 293T cells. Lentiviral particles were collected and used to transduce MRC5 cells. The MRC5-gRNA cells were infected with serial dilution of HCMV in 96-well plates 20 days before quantitative real-time polymerase chain reaction (qRT-PCR) and immunoblot analysis with antibodies. To gain the complete $HCMV_{\Delta UL36}$ strain, the second screen was performed similarly as previously described. The $HCMV_{\Delta UL36}$ single-clone strain was amplified in the MRC5-UL36 cells. The UL36 gRNA target sequence is 5′-CGCACACCTTGAAACGCCGT-3′.

### Plasmids, siRNAs, and transfection

Plasmid construction was described previously (*54*). In brief, the DNA fragment of UL36 was amplified from the HCMV genome and then digested with restriction enzymes (Sal I and Not I, Thermo Fisher Scientific, ER0641 and ER0593) and ligated to the pRK-FLAG vector with T4 ligase (Thermo Fisher Scientific, EP0061). The wild-type pRK-FLAG-UL36 construct was used as a template to generate the mutant UL36 constructs. For Tet-On expression system, the DNA fragment of FLAG-tagged UL36 or mutant was amplified from the corresponding pRK-FLAG-UL36 construct, and then cloned into pLVX-TetOne-Puro. The pRK-FLAG or pRK-HA vectors for cGAS, STING, IRF3, IRF-5D, and TBK1 were previously described (*55*). The pRK-FLAG vectors for IRF3 truncations were generated using the vector for IRF3 as template. The primers are listed in table S1. All mutations were confirmed by DNA sequencing.

Cells were seeded onto the dish 24 hours before z-VAD-FMK, z-IETD-FMK, or z-LEHD-FMK (MCE, HY-16658B, HY-101297, and HY-P1010) treatment or transfection, and plasmids were transiently transfected by using Lipofectamine 2000 reagent (Thermo Fisher Scientific, 11668019) according to the manufacturer′s instruction.

The siRNAs specifically targeting UL36 were synthesized by RiboBio (Guangzhou, China). siRNA (100 nM) was transfected with 3 μl of Lipofectamine 2000 reagent (Thermo Fisher Scientific) and 100 μl of Opti-MEM (Gibco, 22600134) into HFFs cultured in 24-well plates with the confluence of 50 to 70%. Cells were harvested at 24 h.p.i., and total RNAs were extracted. All the primers and oligonucleotides used here are listed in table S1.

### qRT-PCR and ELISA

These experiments were performed as previously described (*55*, *56*). In brief, cells were harvested and total RNA were isolated using a cell total RNA isolation kit (Foregene, RE-03111). The first-strand cDNA was reverse-transcribed with first-strand cDNA Synthesis (Takara, D6110A).). Gene expression was examined with a Bio-Rad SFX connect system by a qRT-PCR SYBR Green Master Mix (Yeasen, 11198ES03). Data were normalized to the expression of the gene encoding β-actin. All the qRT-PCR primers used here are listed in table S1. The assays were conducted using the ABI QuantStudio Q3 real-time PCR system and the data were collected using QuantStudio design and analysis software v1.4. Protein levels of IFN-β (R&D Systems, QK410) and TNFα (Absin Bioscience, abs510006) in samples were measured by standard enzyme-linked immunosorbent assay (ELISA). ELISA was performed using a Synergy H1 microplate reader (BioTek).

### Reporter gene assays

293T cells were transiently transfected with the reporter plasmid (100 ng) and an internal control vector phRL-TK-*Renilla* luciferase (Promega, E1980) (20 ng) together with the indicated plasmids. Empty vector was added to equalize the total amount of DNA. After 24 hours, luciferase assays were performed with a dual-specific luciferase assay kit (Promega, E1980). The firefly luciferase activity was normalized by *Renilla* luciferase to obtain relative luciferase activity.

### Coimmunoprecipitation and immunoblots

These experiments were performed as previously described (*57*). Cells were collected and lysed in lysis buffer containing 20 mM tris-HCl, 150 mM NaCl, 1 mM EDTA, 1% NP-40, and 1% protease and phosphatase inhibitor cocktail (Targetmol, C0002). Cell lysates were subjected to immunoblot analysis with the appropriate antibodies. For immunoprecipitation assays, the lysates were immunoprecipitated with protein G agarose and a control immunoglobulin G (IgG) or the appropriate antibodies (all antibodies used here are listed in table S2) and the precipitants were washed three times with lysis buffer, followed by immunoblot analysis with enhanced chemiluminescence ECL (4A Biotech, BN01036).

### Lentivirus-mediated gene stable expression and Tet-on gene expression

293T cells were transfected with pCDH-FLAG-UL36, pCDH-FLAG-UL36$_{S177T}$, pCDH-FLAG-UL36$_{C131A}$, or the empty vector along with the packaging vectors pSPAX2 and pMD2G. The medium was changed with fresh full medium (10% FBS, 1% streptomycin-penicillin, and 10 μM β-mercaptoethanol) 8 hours post-transfection. After 48 hours, the supernatants were harvested to infect HFFs, followed by puromycin selection for 1 week. For Tet-On inducible gene expression, cells were treated with doxycycline (500 ng/ml; Beyotime, ST039A).

### In vitro pull-down assay

These experiments were performed as previously described (*55*). In brief, the plasmids encoding GST and GST-UL36 were transformed into BL21 competent cells, which were induced with IPTG (1 mM) at 18°C for 16 hours. The cells were lysed in lysis buffer (20 mM tris–HCl, 200 mM NaCl, 5% glycerol, and 0.3% Triton X-100) and the proteins were purified through affinity chromatography using a matrix (Transgen Biotech, DP201–01) followed by glutathione (10 mM in 50 mM tris–HCl) elution and dialysis. 293T cells were transfected with plasmids encoding FLAG-IRF3 or its truncations. Cells were lysed with NP-40 lysis buffer and the cell lysates were immunoprecipitated with anti-FLAG agarose (Sigma-Aldrich, A4596). FLAG-IRF3 or its truncations was obtained by elution with 3×FLAG peptide [100 mg/ml in phosphate-buffered saline (PBS)] (Sigma-Aldrich, SAE0194). The purified GST or GST-UL36 (5 μg) was incubated with FLAG-IRF3 or its truncations at 4°C for overnight followed by glutathione agarose (Transgen Biotech, DP501-01) pull-down for 2 hours in PBS containing protease inhibitors. The glutathione agarose was washed three times with PBS and subject to immunoblot analysis.

### Apoptosis detection assay

HFFs were collected by centrifugation at 1500*g* for 5 min and washed three times with PBS, followed by detection of cell apoptosis using the annexin V–fluorescein isothiocyanate (FITC) apoptosis detection kit (Beyotime, C1062M). Briefly, 195 μl of annexin V–FITC binding solution was added to resuspend cells gently. Then, 5 μl of annexin V–FITC and 10 μl of propidium iodide (PI) staining solution were added, followed by gentle mixing, incubation at room temperature (20 to 25°C) in the dark for 10 to 20 min, and incubation in an ice bath. Flow cytometry analysis was conducted within 1 hour. Early apoptosis: annexin V–FITC single positive, Q3; late apoptosis: annexin V–FITC and PI double positive, Q2; the percentage of apoptotic cells was measured as the sum of Q2 and Q3. This gating strategy was applied to all flow cytometry analyses in this study. The flow cytometry assays were performed using the

LSRFortessa X-20 cell analyzer (BD Biosciences) and the data were analysed using FlowJo v10.6.2.

### Immunofluorescence staining assay

HFFs seeded on the confocal dish were washed three times with PBS and fixed with 3.7% formaldehyde in PBS for 30 min, then permeabilized by 1% Triton X-100 in PBS for 20 min. After blocking with 5% bovine serum albumin (BSA) in PBS for 60 min, cells were incubated with appropriate antibodies diluted in 5% BSA at 4°C overnight. After washing three times with PBS, cells were incubated with Alexa Fluor 488– or Alexa Fluor 594–conjugated IgG (H + L) (ABclonal, AP1177 and AS039) diluted in 5% BSA for 30 min. After washing cells three times with PBS, cell nuclei were stained with DAPI (4′,6-diamidino-2-phenylindole) (Invitrogen, D21490) diluted in PBS for 5 min. Fluorescent signals were detected using a Nikon Eclipse Ti microscope and the images were analyzed with the NIS-Elements Viewer v9.11.02C.

### Statistical analysis

GraphPad Prism (v8.0.2.263) was used for statistical analyses. Sample size and number of repeats are indicated in the respective figure legends. Statistical significance was calculated by one-way or two-way analysis of variance (ANOVA) as indicated in the legends. No animals or data points were excluded from the analyses.

**Correction (10 November 2023):** After publication, the authors alerted the editorial office to an error with the labels in Fig. 4, D and E. In Fig. 4D, the tag names at the top of the panel were swapped. This has been corrected so that HA-IRF3 is the first label with FLAG-STING the second label. In Fig. 4E, "FLAG-IRF3" was mislabeled as "FLAG-STING" on the right side of the figure and has been corrected.

## Supplementary Materials

**This PDF file includes:**

Figs. S1 to S8
Tables S1 and S2

## REFERENCES AND NOTES


1. Y. Cohen, N. Stern-Ginossar, Manipulation of host pathways by human cytomegalovirus: Insights from genome-wide studies. *Semin. Immunopathol.* **36**, 651–658 (2014).
2. P. Griffiths, M. Reeves, Pathogenesis of human cytomegalovirus in the immunocompromised host. *Nat. Rev. Microbiol.* **19**, 759–773 (2021).
3. L. B. Crawford, N. L. Diggins, P. Caposio, M. H. Hancock, Advances in model systems for human cytomegalovirus latency and reactivation. *MBio* **13**, e0172421 (2022).
4. M. R. Wills, E. Poole, B. Lau, B. Krishna, J. H. Sinclair, The immunology of human cytomegalovirus latency: Could latent infection be cleared by novel immunotherapeutic strategies? *Cell. Mol. Immunol.* **12**, 128–138 (2015).
5. S. Manicklal, V. C. Emery, T. Lazzarotto, S. B. Boppana, R. K. Gupta, The "silent" global burden of congenital cytomegalovirus. *Clin. Microbiol. Rev.* **26**, 86–102 (2013).
6. Y. Liu, R. Mu, Y. P. Gao, J. Dong, L. Zhu, Y. Ma, Y. H. Li, H. Q. Zhang, D. Han, Y. Zhang, I. B. McInnes, J. Zhang, B. Shen, G. Yang, Z. G. Li, A cytomegalovirus peptide-specific antibody alters natural killer cell homeostasis and is shared in several autoimmune diseases. *Cell Host Microbe* **19**, 400–408 (2016).
7. T. Crough, R. Khanna, Immunobiology of human cytomegalovirus: From bench to bedside. *Clin. Microbiol. Rev.* **22**, 76–98 (2009).
8. M. Z. Chaudhry, R. Casalegno-Garduno, K. M. Sitnik, B. Kasmapour, A. K. Pulm, I. Brizic, B. Eiz-Vesper, A. Moosmann, S. Jonjic, E. S. Mocarski, L. Cicin-Sain, Cytomegalovirus inhibition of extrinsic apoptosis determines fitness and resistance to cytotoxic CD8 T cells. *Proc. Natl. Acad. Sci. U.S.A.* **117**, 12961–12968 (2020).
9. M. Tarrant-Elorza, C. C. Rossetto, G. S. Pari, Maintenance and replication of the human cytomegalovirus genome during latency. *Cell Host Microbe* **16**, 43–54 (2014).
10. L. Sun, J. Wu, F. Du, X. Chen, Z. J. Chen, Cyclic GMP-AMP synthase is a cytosolic DNA sensor that activates the type I interferon pathway. *Science* **339**, 786–791 (2013).
11. B. Zhong, Y. Yang, S. Li, Y. Y. Wang, Y. Li, F. Diao, C. Lei, X. He, L. Zhang, P. Tien, H. B. Shu, The adaptor protein MITA links virus-sensing receptors to IRF3 transcription factor activation. *Immunity* **29**, 538–550 (2008).
12. W. Sun, Y. Li, L. Chen, H. Chen, F. You, X. Zhou, Y. Zhou, Z. Zhai, D. Chen, Z. Jiang, ERIS, an endoplasmic reticulum IFN stimulator, activates innate immune signaling through dimerization. *Proc. Natl. Acad. Sci. U.S.A.* **106**, 8653–8658 (2009).
13. H. Ishikawa, G. N. Barber, STING is an endoplasmic reticulum adaptor that facilitates innate immune signalling. *Nature* **455**, 674–678 (2008).
14. K. P. Hopfner, V. Hornung, Molecular mechanisms and cellular functions of cGAS-STING signalling. *Nat. Rev. Mol. Cell Biol.* **21**, 501–521 (2020).
15. X. Zhang, X. C. Bai, Z. J. Chen, Structures and mechanisms in the cGAS-STING innate immunity pathway. *Immunity* **53**, 43–53 (2020).
16. Z. Ma, G. Ni, B. Damania, Innate sensing of DNA virus genomes. *Annu. Rev. Virol.* **5**, 341–362 (2018).
17. Z. F. Huang, H. M. Zou, B. W. Liao, H. Y. Zhang, Y. Yang, Y. Z. Fu, S. Y. Wang, M. H. Luo, Y. Y. Wang, Human cytomegalovirus protein UL31 inhibits DNA sensing of cGAS to mediate immune evasion. *Cell Host Microbe* **24**, 69–80.e4 (2018).
18. Y. Z. Fu, Y. Guo, H. M. Zou, S. Su, S. Y. Wang, Q. Yang, M. H. Luo, Y. Y. Wang, Human cytomegalovirus protein UL42 antagonizes cGAS/MITA-mediated innate antiviral response. *PLOS Pathog.* **15**, e1007691 (2019).
19. Y.-Z. Fu, S. Su, H.-M. Zou, Y. Guo, S.-Y. Wang, S. Li, M.-H. Luo, Y.-Y. Wang, Human cytomegalovirus DNA polymerase subunit UL44 antagonizes antiviral immune responses by suppressing IRF3- and NF-κB-mediated transcription. *J. Virol.* **93**, e00181-19 (2019).
20. Y. Z. Fu, S. Su, Y. Q. Gao, P. P. Wang, Z. F. Huang, M. M. Hu, W. W. Luo, S. Li, M. H. Luo, Y. Y. Wang, H. B. Shu, Human cytomegalovirus tegument protein UL82 inhibits STING-mediated signaling to evade antiviral immunity. *Cell Host Microbe* **21**, 231–243 (2017).
21. M. Biolatti, V. Dell'Oste, S. Pautasso, F. Gugliesi, J. von Einem, C. Krapp, M. R. Jakobsen, C. Borgogna, M. Gariglio, M. de Andrea, S. Landolfo, Human cytomegalovirus tegument protein pp65 (pUL83) dampens type I interferon production by inactivating the DNA sensor cGAS without affecting STING. *J. Virol.* **92**, e01774-17 (2018).
22. H. M. Zou, Z. F. Huang, Y. Yang, W. W. Luo, S. Y. Wang, M. H. Luo, Y. Z. Fu, Y. Y. Wang, Human cytomegalovirus protein UL94 targets MITA to evade the antiviral immune response. *J. Virol.* **94**, e00022-20 (2020).
23. J. Paijo, M. Döring, J. Spanier, E. Grabski, M. Nooruzzaman, T. Schmidt, G. Witte, M. Messerle, V. Hornung, V. Kaever, U. Kalinke, cGAS senses human cytomegalovirus and induces type i interferon responses in human monocyte-derived cells. *PLOS Pathog.* **12**, e1005546 (2016).
24. X. Cai, Y. H. Chiu, Z. J. Chen, The cGAS-cGAMP-STING pathway of cytosolic DNA sensing and signaling. *Mol. Cell* **54**, 289–296 (2014).
25. M. H. Orzalli, J. C. Kagan, Apoptosis and necroptosis as host defense strategies to prevent viral infection. *Trends Cell Biol.* **27**, 800–809 (2017).
26. H. Everett, G. McFadden, Apoptosis: An innate immune response to virus infection. *Trends Microbiol.* **7**, 160–165 (1999).
27. S. G. Verburg, R. M. Lelievre, M. J. Westerveld, J. M. Inkol, Y. L. Sun, S. T. Workenhe, Viral-mediated activation and inhibition of programmed cell death. *PLOS Pathog.* **18**, e1010718 (2022).
28. S. W. Tait, D. R. Green, Mitochondria and cell death: Outer membrane permeabilization and beyond. *Nat. Rev. Mol. Cell Biol.* **11**, 621–632 (2010).
29. M. O. Hengartner, The biochemistry of apoptosis. *Nature* **407**, 770–776 (2000).
30. L. Galluzzi, C. Brenner, E. Morselli, Z. Touat, G. Kroemer, Viral control of mitochondrial apoptosis. *PLOS Pathog.* **4**, e1000018 (2008).
31. G. V. Putcha, C. A. Harris, K. L. Moulder, R. M. Easton, C. B. Thompson, E. M. Johnson Jr., Intrinsic and extrinsic pathway signaling during neuronal apoptosis: Lessons from the analysis of mutant mice. *J. Cell Biol.* **157**, 441–453 (2002).
32. C. A. Benedict, P. S. Norris, C. F. Ware, To kill or be killed: Viral evasion of apoptosis. *Nat. Immunol.* **3**, 1013–1018 (2002).
33. M. B. Reeves, A. Breidenstein, T. Compton, Human cytomegalovirus activation of ERK and myeloid cell leukemia-1 protein correlates with survival of latently infected cells. *Proc. Natl. Acad. Sci. U.S.A.* **109**, 588–593 (2012).
34. M. A. Peppenelli, K. C. Arend, O. Cojohari, N. J. Moorman, G. C. Chan, Human cytomegalovirus stimulates the synthesis of select Akt-dependent antiapoptotic proteins during viral entry to promote survival of infected monocytes. *J. Virol.* **90**, 3138–3147 (2016).
35. W. A. Hayajneh, A. M. Colberg-Poley, A. Skaletskaya, L. M. Bartle, M. M. Lesperance, D. G. Contopoulos-Ioannidis, N. L. Kedersha, V. S. Goldmacher, The sequence and antiapoptotic functional domains of the human cytomegalovirus UL37 exon 1 immediate early protein are conserved in multiple primary strains. *Virology* **279**, 233–240 (2001).
36. V. S. Goldmacher, vMIA, a viral inhibitor of apoptosis targeting mitochondria. *Biochimie* **84**, 177–185 (2002).

37. A. Skaletskaya, L. M. Bartle, T. Chittenden, A. L. McCormick, E. S. Mocarski, V. S. Goldmacher, A cytomegalovirus-encoded inhibitor of apoptosis that suppresses caspase-8 activation. *Proc. Natl. Acad. Sci. U.S.A.* **98**, 7829–7834 (2001).
38. A. Rajput, A. Kovalenko, K. Bogdanov, S. H. Yang, T. B. Kang, J. C. Kim, J. du, D. Wallach, RIG-I RNA helicase activation of IRF3 transcription factor is negatively regulated by caspase-8-mediated cleavage of the RIP1 protein. *Immunity* **34**, 340–351 (2011).
39. L. Cicin-Sain, Z. Ruzsics, J. Podlech, I. Bubić, C. Menard, S. Jonjić, M. J. Reddehase, U. H. Koszinowski, Dominant-negative FADD rescues the in vivo fitness of a cytomegalovirus lacking an antiapoptotic viral gene. *J. Virol.* **82**, 2056–2064 (2008).
40. L. Ebermann, Z. Ruzsics, C. A. Guzmán, N. van Rooijen, R. Casalegno-Garduño, U. Koszinowski, L. Čičin-Šain, Block of death-receptor apoptosis protects mouse cytomegalovirus from macrophages and is a determinant of virulence in immunodeficient hosts. *PLOS Pathog.* **8**, e1003062 (2012).
41. C. Ménard, M. Wagner, Z. Ruzsics, K. Holak, W. Brune, A. E. Campbell, U. H. Koszinowski, Role of murine cytomegalovirus US22 gene family members in replication in macrophages. *J. Virol.* **77**, 5557–5570 (2003).
42. C. E. Patterson, T. Shenk, Human cytomegalovirus UL36 protein is dispensable for viral replication in cultured cells. *J. Virol.* **73**, 7126–7131 (1999).
43. A. L. McCormick, L. Roback, D. Livingston-Rosanoff, C. St Clair, The human cytomegalovirus UL36 gene controls caspase-dependent and -independent cell death programs activated by infection of monocytes differentiating to macrophages. *J. Virol.* **84**, 5108–5123 (2010).
44. P. Li, H. Jiang, H. Peng, W. Zeng, Y. Zhong, M. He, L. Xie, J. Chen, D. Guo, J. Wu, C. M. Li, Non-structural protein 5 of Zika virus interacts with p53 in human neural progenitor cells and induces p53-mediated apoptosis. *Virol. Sin.* **36**, 1411–1420 (2021).
45. Y. Ren, T. Shu, D. Wu, J. Mu, C. Wang, M. Huang, Y. Han, X. Y. Zhang, W. Zhou, Y. Qiu, X. Zhou, The ORF3a protein of SARS-CoV-2 induces apoptosis in cells. *Cell. Mol. Immunol.* **17**, 881–883 (2020).
46. C. Liang, B. H. Oh, J. U. Jung, Novel functions of viral anti-apoptotic factors. *Nat. Rev. Microbiol.* **13**, 7–12 (2015).
47. Y. Ren, A. Wang, D. Wu, C. Wang, M. Huang, X. Xiong, L. Jin, W. Zhou, Y. Qiu, X. Zhou, Dual inhibition of innate immunity and apoptosis by human cytomegalovirus protein UL37x1 enables efficient virus replication. *Nat. Microbiol.* **7**, 1041–1053 (2022).
48. F. Marino-Merlo, E. Papaianni, M. A. Medici, B. Macchi, S. Grelli, C. Mosca, C. Borner, A. Mastino, HSV-1-induced activation of NF-κB protects U937 monocytic cells against both virus replication and apoptosis. *Cell Death Dis.* **7**, e2354 (2016).
49. L. Jin, W. Peng, G. C. Perng, D. J. Brick, A. B. Nesburn, C. Jones, S. L. Wechsler, Identification of herpes simplex virus type 1 latency-associated transcript sequences that both inhibit apoptosis and enhance the spontaneous reactivation phenotype. *J. Virol.* **77**, 6556–6561 (2003).
50. A. Slonchak, L. E. Hugo, M. E. Freney, S. Hall-Mendelin, A. A. Amarilla, F. J. Torres, Y. X. Setoh, N. Y. G. Peng, J. D. J. Sng, R. A. Hall, A. F. van den Hurk, G. J. Devine, A. A. Khromykh, Zika virus noncoding RNA suppresses apoptosis and is required for virus transmission by mosquitoes. *Nat. Commun.* **11**, 2205 (2020).
51. C. Gubser, D. Bergamaschi, M. Hollinshead, X. Lu, F. J. M. van Kuppeveld, G. L. Smith, A new inhibitor of apoptosis from vaccinia virus and eukaryotes. *PLOS Pathog.* **3**, e17 (2007).
52. S. T. Wasilenko, T. L. Stewart, A. F. Meyers, M. Barry, Vaccinia virus encodes a previously uncharacterized mitochondrial-associated inhibitor of apoptosis. *Proc. Natl. Acad. Sci. U.S.A.* **100**, 14345–14350 (2003).
53. M. A. Salako, M. J. Carter, G. E. Kass, Coxsackievirus protein 2BC blocks host cell apoptosis by inhibiting caspase-3. *J. Biol. Chem.* **281**, 16296–16304 (2006).
54. T. Shu, M. Huang, D. Wu, Y. Ren, X. Zhang, Y. Han, J. Mu, R. Wang, Y. Qiu, D. Y. Zhang, X. Zhou, SARS-coronavirus-2 Nsp13 possesses NTPase and RNA helicase activities that can be inhibited by bismuth salts. *Virol. Sin.* **35**, 321–329 (2020).
55. B. Lu, Y. Ren, X. Sun, C. Han, H. Wang, Y. Chen, Q. Peng, Y. Cheng, X. Cheng, Q. Zhu, W. Li, H. L. Li, H. N. du, B. Zhong, Z. Huang, Induction of INKIT by viral infection negatively regulates antiviral responses through inhibiting phosphorylation of p65 and IRF3. *Cell Host Microbe* **22**, 86–98.e4 (2017).
56. Y. Fang, Z. Liu, Y. Qiu, J. Kong, Y. Fu, Y. Liu, C. Wang, J. Quan, Q. Wang, W. Xu, L. Yin, J. Cui, Y. Xu, S. Curry, S. Jiang, L. Lu, X. Zhou, Inhibition of viral suppressor of RNAi proteins by designer peptides protects from enteroviral infection in vivo. *Immunity* **54**, 2231–2244.e6 (2021).
57. Y. Ren, Y. Zhao, D. Lin, X. Xu, Q. Zhu, J. Yao, H. B. Shu, B. Zhong, The type I interferon-IRF7 axis mediates transcriptional expression of Usp25 gene. *J. Biol. Chem.* **291**, 13206–13215 (2016).


**Acknowledgments:** We thank Y.-Z. Fu, Y.-Y. Wang, and B. Zhong (Wuhan, China) for reagents. We thank all members of the Zhou laboratory for their support. We would like to thank the staff from Center for Instrumental Analysis and Metrology, Wuhan Institute of Virology, CAS for technical assistance. **Funding:** This work was supported by National Key R&D Program of China grant 2021YFC2300700 (X.Z.); National Natural Science Foundation of China grants 32225004 (X.Z.), 32100106 (Y.R.), and U21A20423 (X.Z.); Hubei Provincial Natural Science Foundation grant 2023AFB582 (Y.R.); and CAS Youth Innovation Promotion Association grant 2023351 (Y.R.).
**Author contributions:** Performing most experiments: Y.R. Performing specific experiments: A. W., B.Z., W.J., X.-X.Z., J.L., M.H., and Y.Q. Conceptualization, designing experiments, and analyzing data: Y.R. and X.Z. Supervision: X.Z. Writing: Y.R. and X.Z. **Competing interests:** The authors declare that they have no competing interests. **Data and materials availability:** All data needed to evaluate the conclusions in the paper are present in the paper and/or the Supplementary Materials.

Submitted 10 May 2023
Accepted 31 August 2023
Published 4 October 2023
10.1126/sciadv.adi6586